Inversion of Residual Gravity Anomalies using Tuned-PSO Technique

Ravi Roshan and Upendra Kumar Singh
Department of Applied Geophysics, Indian School of Mines, Dhanbad – 826 004, India
Correspondence: roshanravi.sinha@gmail.com

Abstract

Many kinds of particle swarm optimization (PSO) technique are now available and various efforts have been made to solve linear and non linear problems as well as one dimensional and multidimensional problem of geophysical data. Particle swarm optimization is a Meta heuristic optimization method that requires the intelligent guess and suitable selection of controlling parameters (i.e. Inertia weight and acceleration coefficient) for better convergence at global minima. The proposed technique Tuned–PSO is an improved technique of PSO, in which effort has been made for choosing the controlling parameters and these parameters have selected after analysing the response of various possible exercises using synthetic gravity anomalies over various geological sources. The applicability and efficacy of the proposed method is tested and also validated using synthetic gravity anomalies over various source geometries. Finally Tuned-PSO is applied over field residual gravity anomalies of two different geological terrains to find out the model parameters namely amplitude coefficient factor (A), shape factor (q) and depth (z). The analysed results have been compared with published results obtained by different methods that show a significantly excellent agreement with real model parameters. The results also show that the proposed approach is not only superior to the other methods but also shows that the strategy has enhanced the exploration capability of proposed method. Thus Tuned-PSO is an efficient and more robust technique to achieve optimal solution with minimal error.

Keywords: Tuned–PSO, gravity anomalies, inversion.

1. Introduction

Gravity method is based on the measurement of gravity anomalies caused by the density variation due to source anomalies. Gravity method has been used in a wide range of application as a reconnaissance method for oil exploration and as a secondary method for mineral exploration, to find out the approximate geometry of the source anomalies, bedrock depths, and shapes of the earth. Interpretation of geophysical data that involves solving an

inverse problem; many techniques have been developed to invert the geophysical data to estimate the model parameters. These methods can be broadly categorised into two groups: (1) local search technique (e.g. Steepest descent method; conjugate gradient method, ridge regression, Levenberg- Marquardt method etc.) and (2) global search techniques (e.g., simulated annealing, genetic algorithms, particle swarm optimization, Ant colony optimization etc.) Local search technique is simple and requires a very good initial presumption – close to true model for a successful convergence. In other hand global search method may provide an acceptable solution but computationally time intensive. There are several local and global inversion technique has been developed to interpret gravity anomalies (Thanassoulas *et al.*, 1987; Shamsipour *et al.*, 2012; Montesinos *et al.*, 2005; Qiu, 2009; Toushmalani, 2013). However, PSO has been successfully applied in many fields, such as model construction, biomedical images, electromagnetic optimization, hydrological problem etc. (Cedeno and Agrafiotis, 2003; Wachowiak *et al*., 2004; Boeringer and Werner, 2004; Kumar and Reddy, 2007; Eberhart and Shi, 2001; El-Kaliouby and Al-Garni, 2009) but in the geophysical field PSO has limited number of applications (Alvarez et al., 2006; Shaw and Srivastava, 2007).

In this paper improved Particle Swarm Optimization known as Tuned-PSO with fine tuning of learning parameters have been tested using synthetic gravity anomalies over kinds of geometrical bodies and compared their efficacy. On the basis of performance, finally Tuned PSO has been used to invert gravity anomalies to find out the essential model parameters such as shape factor (q), depth (z), amplitude coefficient factor (A) and horizontal location of the source geometry.

2. Forward modelling for generating the synthetic gravity anomalies

A general expression of gravity anomaly caused by a sphere, an infinite long horizontal cylinder and a semi-infinite vertical cylinder have been used for generating the gravity anomalies in forward problem that is given in equation 1 (Abdelrahman *et al*., 1989) as follows:

$$g(x_i, z, q) = A\frac{z^m}{(x_i^2 + z^2)^q} \quad (1)$$

Where

$$A=\begin{cases}\frac{4}{3}\pi G\sigma R^3, & \text{for a sphere,}\\ 2\pi G\sigma R^2, & \text{for a horizontal cylinder,}\\ \pi G\sigma R^2, & \text{for a vertical cylinder,}\end{cases} \qquad m=\begin{cases}1,\\ 1,\\ 0,\end{cases}$$

$$q=\begin{cases}\frac{3}{2} & \text{for a sphere,}\\ 1 & \text{for a horizontal cylinder,}\\ \frac{1}{2} & \text{for a vertical cylinder; R} << \text{z.}\end{cases}$$

Where A, q and z represent amplitude coefficient factor, shape factor and depth respectively; and x_i, σ, G and R are the position coordinate, density contrast, universal gravitational constant and radius of geometrical bodies respectively. Two types of synthetic gravity data have been created over spherical and vertical cylindrical geometrical model using forward modelling of the equation 1. The value of parameters for spherical model i.e. Amplitude coefficient factor (A), shape factor and depth have been taken 600 mGal*km^2, 1.5 and 5.0 km respectively. Similarly, the value of parameters for vertical cylindrical model (A = 200 mGal*km, q = 0.5 and z = 3.0 km) have been selected. The shape factor approaches to zero as the structure becomes a nearly horizontal bed and approaches 1.5 as the structure becomes a perfect sphere (point mass). As in the formulae x_i is the position coordinate; at the origin x_i = 0 then equation 1 becomes,

$$g(0)=\frac{A}{z^{2q-m}} \tag{2}$$

The equation 3 is taken for addition of 10% white Gaussian noise.

$$g_{noisy}(x)=awgn(g(x),0.1) \tag{3}$$

3. Tuned- Particle Swarm Optimization (Tuned-PSO)

Tuned-Particle Swarm Optimization (Tuned-PSO) is an improved Particle swarm optimization (PSO) method after the fine tuning of its learning parameters. The concept of PSO is described as follows (Eberhart and Kennedy, 1995): (a) each potential solution called as particles and knows its best values so far (P_{best}) and its position more over each particle

knows the best value in the group (G_{best}) among the P_{best}. All of the best values are based on objective function (Q) for each problem to be solved. Each particle tries to modify its position through the current velocity and its positions. The velocity of each particle can be updated using the following equations (Santos, 2010):

$$v_i^{k+1} = \omega^k v_i^k + c_1 rand() * \left(P_{best-i}^k - x_i^{k+1}\right) + c_2 rand() * \left(G_{best}^k - x_i^{k+1}\right)$$

$$x_i^{k+1} = x_i^k + v_i^{k+1} \quad (4)$$

Where v_i^k is the velocity of i_{th} particle at k_{th} iteration, x_i^k represents current position of i_{th} particle at k_{th} iteration, $rand()$ is a random number in the range of 0 and 1. c_1 & c_2 are constants known as cognitive coefficient and social coefficient respectively. The coefficient c_1 has contribution towards the self exploration of a particle and the coefficient c_2 has a contribution towards the motion of the particles in global direction, and ω is an inertia weight in the range [0, 1]. The objective function has calculated by following equation (Santos, 2010).

$$Q = \frac{2\sum_i^N |V_i^o - V_i^c|}{\sum_i^N |V_i^o - V_i^c| + \sum_i^N |V_i^o + V_i^c|} \quad (5)$$

Where N is the number of iteration, v_i^o and v_i^c are observed and calculated gravity anomaly measured at point $p(x_i)$ respectively.

4 Discussion and Results

4.1 *Selection of learning parameter for Tuned-PSO Modelling*

In this paper, a judicious selection of the parameters (i.e. ω, c_1, and c_2,) has been discussed for controlling the convergence behaviours of Tuned-PSO based algorithm. The settings of these parameters determine how it optimizes the search-space. These algorithms with suitable selection of parameter become more powerful global search algorithm for their practical applications.

4.1.1 *Inertia weight*

Inertia weight ω controls the momentum of the particle (Eberhart and Shi, 2001; Eberhart and Kennedy, 1995). Here two kinds of source geometry are adopted to evaluate more suitable ranges of parameters in the Tuned-PSO. For tuning of inertia weight, 0, 0.4, 0.7, 0.9, has been taken for two different acceleration coefficients at 1.4 and 2.0 respectively. From Figure 1 & Table 1, it is clear that the best convergence has performed by algorithm at inertia weight 0.7. This value of inertia weight produces high convergence rate at less number of iteration than the other values.

4.1.2 The maximum velocity v_{max}

The maximum velocity v_{max} determines the maximum change one particle can undergo in its positional coordinates during iteration and used to avoid explosion and divergence. Usually, the full search ranges of the particle's positions as the v_{max} are fixed. For example, in case, a particle has position vector $x = (x_1, x_2, x_3)$ and if $-15 <= x_i <= 15$ for i=1, 2 and 3, then $v_{max} = 30$ is fixed.

4.1.3 *The swarm size*

It is quite a common practice in the PSO literature to limit the range of number of particles. Van den Bergh and Engelbrecht have shown that though there is a slight improvement of the optimal value with increasing swarm size, a larger swarm increases the number of function evaluations to converge to an error limit. However, Eberhart and Shi Illustrated that the population size has hardly any effect on the performance of the PSO method. So, in this paper population size has taken 100.

4.1.4 *The acceleration coefficients c_1 and c_2*

To find the best tuning of learning parameters, various values of c_1, c_2 (i.e. $c_1 = c_2 = 1.0$, 1.2, 1.4, 1.6, 1.8, and 2.0) and inertia weights (i.e. 0.4, 0.7 and 0.9) are taken, and various exercises have been made using the two different geometrical bodies by fixing the each of the inertia weight (Table 1). The results was analysed and found that more suitable values of c_1 and c_2 (i.e. $c_1 = c_2 = 1.4$) are the best tuned acceleration coefficients for our case. These values of acceleration coefficients have been used to invert the gravity anomalies, which provide significant improvement and produce optimal solutions of the geological bodies.

4.2 *Application to Synthetic gravity anomalies*

Initially two geometrical models i.e. sphere and vertical cylinder has been considered for testing the applicability and efficacy of Tuned-PSO. The synthetic gravity anomalies over above considered models are generated from equation (1). In Addition, other data sets (noisy synthetic gravity anomalies) are also generated with 10% Gaussian noise to perceive the efficacy of proposed algorithm. In each case, the gravity profile length is 51 km and data points are kept at equal interval of one km. The proposed Tuned-PSO algorithm has been applied on above synthetic data sets. The optimized results obtained by Tuned-PSO for synthetic data without noise have been shown in Table 1(a) and Table 2(a). Similarly, the results for synthetic data with noise have been shown in Table 1(b) and Table 2(b).

Figure 1 shows the iteration versus error. This figure 1 suggests that error is minimum and having less number of local minima at values of controlling parameters c_1=1.4, c_2=1.4 and w= 0.7. It means that the Tuned-PSO technique minimise the number of local minima for solving the geophysical nonlinear inverse problems. The synthetic gravity anomaly without noise and computed gravity anomaly by Tuned-PSO are shown in Figure 2(a) and 3(a) respectively. Similarly, Synthetic gravity anomaly with noise and computed gravity anomaly by Tuned PSO has shown in Figure 2(b) and 3(b). Figure 2(a) and Figure 3(a) show that the calculated gravity anomalies curves by Tuned-PSO is matched well with the synthetic gravity anomaly curves for spherical and vertical cylindrical model respectively. The behaviour of p_{best} and g_{best} are shown in Figure 4 that suggests the error for g_{best} decreases more rapidly with high convergence rate.

Table 2(a) and Table 3(a) show the values of RMS error using the synthetic data without noise. Also Table 2(b) and Table 3(b) show the RMS error using the synthetic data with noise. The analysis of above tables reflects that the RMS error is comparatively higher in the case of synthetic data with noise. However, the horizontal location (x_0) is a substantially stable parameter and varies in a small scale.

4.3 *Application to Field gravity anomalies*

4.3.1. *Mobrun Sulphide Body, Near Rouyn- Noranda, Canada*

Mobrun polymetallic deposit near Rouyn- Noranda comprises two complexes of massive lenses within mainly felsic volcanic rocks of the Archean Blake River Group (Barrett. *et al.*, 1992). Host volcanic rocks of main sulphide ore body are mostly massive, breciated, and tuffaceous rhyolites. Mobrun ore body is located at shallow depth; top of the body approximately 17 m depth and extended to 175 m. (Aghajani et al., 2009)

Tuned-PSO in MATLAB environment has been applied to field residual gravity anomaly. The anomaly profile length of 268 m has been taken from the Mobrun sulphide body, Noranda, Canada (Nettleton, 1976; Essa, 2012). It is seen from Figure 5 that both anomalies curves i.e. analysed from Tuned-PSO and observed gravity anomalies are significantly well correlated with optimal RMS error of 0.0271%. The results in terms of model parameters (amplitude coefficient factor, shape factor and depth) over the Mobrun ore body analysed from Tuned-PSO method can seen in Table 4(a). This table provides the optimum results obtained from Tuned-PSO with 0.0271% error agrees well with the results obtained from other methods. The calculated value of shape factor, q is 0.77 (Table 4a). This value over Mobrun sulphide ore body reflects the shape of a semi-infinite vertical cylindrical

geological body is present at depth of 30 m. Since the shape factor computed by proposed method (q = 0.77) lies between the shape factor of a perfect semi-infinite vertical cylinder i.e. q = 0.5 and the shape factor of an infinite horizontal cylinder i.e. q = 1.0. It can be seen from Table 4(b), the values of amplitude coefficient factor, shape factor and depth correspond to 60.0, 0.77 and 30 are more accurate than the results analysed by various authors.

4.3.2. *Louga Anomaly West coast of Senegal, West Africa*

The study area Louga anomaly of west coast of Senegal is taken for another case study for interpretation of gravity data using Tuned –PSO. The Senegal basin is part of the north-west African coastal basin- a typical passive margin basin opening west to the Atlantic. The complexities of the rift tectonics of the Atlantic opening gave rise to a series of sub-basins aligned north-south. The pre-rift (Upper Proterozoic to Palaeozoic), syn-rift (Permian to Lower Jurassic) and post-rift are divided into a number of sub-basins, controlled by east west transform related lineaments (Nettleton, 1962).

In this paper Tuned-PSO in MATLAB environment has been also applied to another field case study. Gravity anomaly of Louga area, West coast of Senegal, West Africa (Essa, 2014) has taken for Tuned- PSO analysis as shown in Figure 6 has Profile length 32 km. The results in terms of model parameters (amplitude coefficient factor, shape factor and depth) over the Louga anomaly analysed from Tuned-PSO method can be seen in Table 5(a). It is seen from Figure 6 that both gravity anomalies curves analysed from Tuned-PSO and observed gravity anomalies are extremely well correlated with optimal RMS error of 0.0271%. The optimum results of model parameters amplitude coefficient factor (A), shape factor (q) and depth (z) are 545.30 mGal*km, 0.53 and 4.92 km respectively that shows significantly good agreement with the results obtained by various authors as shown in Table 5(b). The Tuned PSO analysed value of shape factor confirms that the shape of the causative body is semi-infinite vertical cylindrical body present at depth about 4.92 km.

5. Conclusions

In this paper, various synthetic gravity anomalies and field gravity anomalies have been adopted for evaluating the applicability and efficacy of Tuned-PSO algorithms and also determining the suitable ranges of learning parameters setting (i.e. inertia weight and acceleration coefficients). On the basis of the performance, a novel algorithm PSO with suitable learning parameters has been implemented to gravity anomalies of assuming models such as sphere and vertical cylinder. This technique has been tested and demonstrated on

synthetic gravity anomalies with and without Gaussian noise and finally applied to field residual gravity anomalies over Mobrun sulphide ore body, Noranda, QC, Canada and Louga Anomaly of West coast of Senegal, West Africa. This technique provides robust and plausible results even in the presence of noise that are consistent with the results obtained from other classical methods. Thus Tuned PSO technique is powerful tool that improves the results of classical PSO and other technique significantly with less time and optimal error.

6. References

Abdelrahman, E.M., Bayoumi, A.I., Abdelhady, Y.E., Gobashy, M.M., El-Araby, H.M., 1989. Gravity interpretation using correlation factors between successive least-squares residual anomalies. Geophysics, 54, 1614-1621.

Aghajani, Hamid., Moradzadeh, Ali., Zeng, Hualin., 2009. Normalized full gradient of gravity anomaly method and its application to the Mobrun Sulfide Body, Canada. World Applied Science Journal, 6(3), 393-400.

Alvarez, J.P.F., Marti`nez, F., Gonzalo, E.G., Pe`rez, C.O.M., 2006. Application of the particle swarm optimization algorithm to the solution and appraisal of the vertical electrical sounding inverse problem. In: proceedings of the 11th Annual Conference of the international Association of Mathematical Geology (IAMG06), Li_ege, Belgium, CDROM.

Barrett, T.J., Cattalani, S., Holy, L., Riopel, J., Lafleur, P.J., 1992. Massive sulphide deposits of the Noranda area, Quebec .IV. The Mobrun mine. Canadian Journal of Earth Science, 29(7), 1349-1374, 10.1139/e92-110.

Boeringer, D.W., Werner, D.H., 2004. Particle swarm optimization versus genetic algorithms for phased array synthesis. IEEE Transactions on Antennas and Propagation, 52, 771–779.

Cedeno, W., Agrafiotis, D.K., 2003. Using particle swarms for the development of QSAR models based on K-nearest neighbour and kernel regression. Journal of Computer Aided Molecular Design, 17, 255–263.

Eberhart, R.C., Kennedy, J., 1995. A new optimizer using particle swarm theory. In: proceedings of the IEEE The sixth Symposium on Micro Machine and Human Centre, Nagoya, Japan, 39-43.

Eberhart, R.C., Shi, Y., 2001. Particle swarm optimization: developments, applications and resources. In: Proceedings of the Congress on Evolutionary Computation, Seoul, Korea, 81–86.

267 El-Kaliouby, H.M., Al-Garni, M.A., 2009. Inversion of self-potential anomalies caused by
268 2D inclined sheets using neural networks. Journal of Geophysics and Engineering, 6,
269 29–34. doi:10.1088/1742-2132/6/1/003.
270 Essa, K. S., 2007. Gravity data interpretation using s-curves method. Journal of Geophysical
271 Engineering, 4, 204–13.
272 Essa, K.S., 2012. A fast interpretation method for inverse modelling or residual gravity
273 anomalies caused by simple geometry. Journal of Geophysical research, Article ID
274 327037, 10 pages.doi:10.1155/2012/327037.
275 Essa, K.S., 2014. New fast least squares algorithm for estimating the best fitting parameters
276 dut to simple geometric structures from gravity anomalies. Journal of Advanced
277 research, 5, 57-67.
278 Montesinos, F.G., Arnoso, j., Vieira, R., 2005. Using a genetic algorithm for 3-D inversion
279 of gravity data in Fuerteventura (Canary Island). International Journal of Earth
280 Sciences (Geol Rundsch), 94, 301-316.
281 Nettleton, L.L., 1976. Gravity and magnetic in oil prospecting. New York: McGraw-Hill
282 Book Co., 480.
283 Nettleton, LL. Gravity and magnetics for geologists and seismologists. AAPG Bull 1962, 46,
284 1815–38.
285
286 Qiu, N., Liu, Q., Gao, Q., 2009. Gravity Data inversion based genetic algorithm and
287 Generalized least square. 978-1-4244-4738-1/09/$25.00 ©2009 IEEE
288 Roy, L., Agarwal, B.N.P., Shaw, R.K., 2000. A new concept in Euler deconvolution of
289 isolated gravity anomalies. Geophysical prospecting, 48, 3, 559-575.
290 Santos, F.A.M., 2010. Inversion of self – potential of idealized bodies' anomalies using
291 particle swarm optimization. Computers and Geosciences, 36, 1185-1190.
292 Shamsipour, P., Marcotte, D., Chouteau, M., 2012. 3D stochastic Joint Inversion of gravity
293 and magnetic data. Journal of Applied Geophysics, 79, 27-37.
294 Shaw, R., Srivastava, S., 2007. Particle swarm optimization: a new tool to invert geophysical
295 data. Geophysics, 72(2), 75-83.
296 Thanassoulas, C., Tselentis, G.-A., Dimitriadis, K., 1987. Gravity inversion of a fault by
297 Marquardt's Method. Computer and Geosciences, 13, 399-404.
298 Toushmalani, R., 2013. Comparision result of inversion of gravity data of a fault by particle
299 swarm optimization and Levenberg-Marquardt methods. SpringerPlus, 2, 462.

Wachowiak, M.P., Smoli`kova`, R., Zheng, Y., Zurada, J.M., Elmaghraby, A.S., 2004. An approach to multimodal biomedical image registration utilizing particle swarm optimization. IEEE Transaction on Evolutionary Computation, 8(3), 289-301.

Figure and Table Captions

Figure 1. Iteration versus RMS error plot at different acceleration coefficients and inertia weights.

Figure 2. (a) Synthetic gravity anomaly versus Tuned-PSO calculated gravity anomaly over spherical model and (b) Synthetic gravity anomaly versus Tuned-PSO calculated gravity anomaly over same model with 10% white gaussian noise.

Figure 3. (a) Synthetic gravity anomaly versus Tuned-PSO calculated gravity anomaly over vertical cylindrical model, (b) Synthetic gravity anomaly versus Tuned-PSO calculated gravity anomaly over same model with 10% white gaussian noise.

Figure 4. Iteration versus RMS error of Tuned-PSO showing p_{best} and g_{best} over synthetic gravity anomaly.

Figure 5. Observed field gravity anomaly versus Tuned-PSO calculated gravity anomaly over Mobrun sulphide ore body, Canada.

Figure 6. Observed field gravity anomaly versus Tuned-PSO calculated gravity anomaly over West Senegal anomaly, Louga area, South Africa.

Table 1. Performance of the acceleration coefficients c_1 and c_2 using the synthetic gravity anomalies over spherical and vertical cylindrical geometrical bodies.

Table 2. (a) Optimized model parameters, converged iteration and RMS error in the inversion of synthetic gravity anomaly over a spherical source model and (b) optimized parameters, converged iteration and RMS error in the inversion of synthetic gravity anomaly with 10% white gaussian noise over a same source model from Tuned-PSO.

Table 3. (a) Optimized model parameters, converged iteration and RMS error in the inversion of synthetic gravity anomaly over a vertical cylindrical source model and (b) optimized parameters, converged iteration and RMS error in the inversion of synthetic gravity anomaly with 10% white gaussian noise over a same source model from Tuned-PSO.

Table 4. (a) Analysed results and parameters (A, z and q) used to invert the gravity anomaly over Mobrun sulphide ore body and (b) comparative results over Mobrun field, Canada from various methods and Tuned- PSO.

Table 5. (a) Analysed results and parameters (A, z and q) used to invert the gravity anomaly over West Senegal anomaly, Louga area, South Africa and (b) comparative results over same area from various methods and Tuned- PSO.

Figure 1

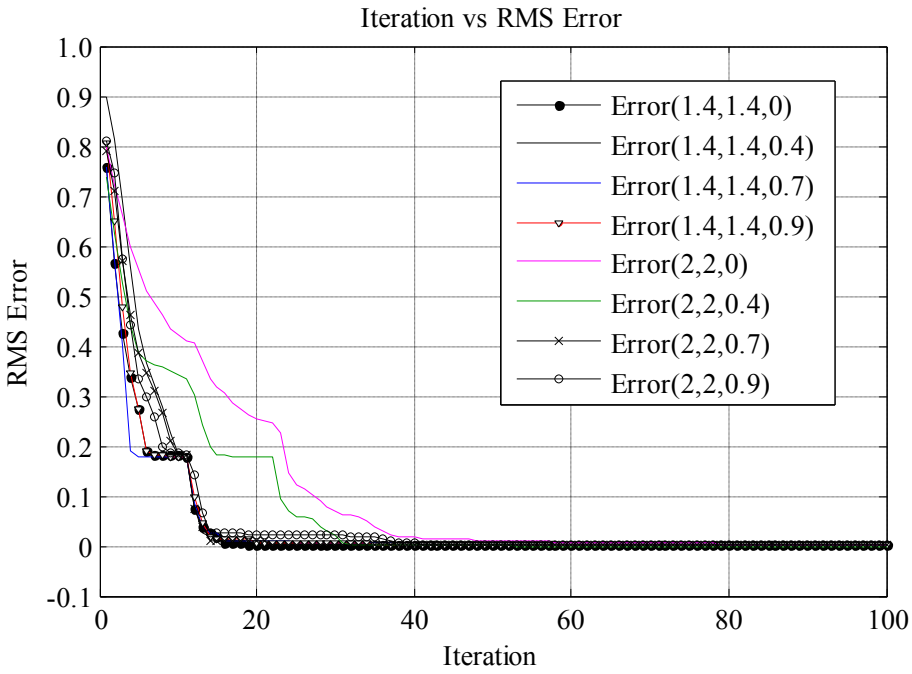
Iteration vs RMS Error
RMS Error
Iteration
1.0
0.9
0.8
0.7
0.6
0.5
0.4
0.3
0.2
0.1
0
-0.1
0
20
40
60
80
100
Error(1.4,1.4,0)
Error(1.4,1.4,0.4)
Error(1.4,1.4,0.7)
Error(1.4,1.4,0.9)
Error(2,2,0)
Error(2,2,0.4)
Error(2,2,0.7)
Error(2,2,0.9)

Figure 2(a)

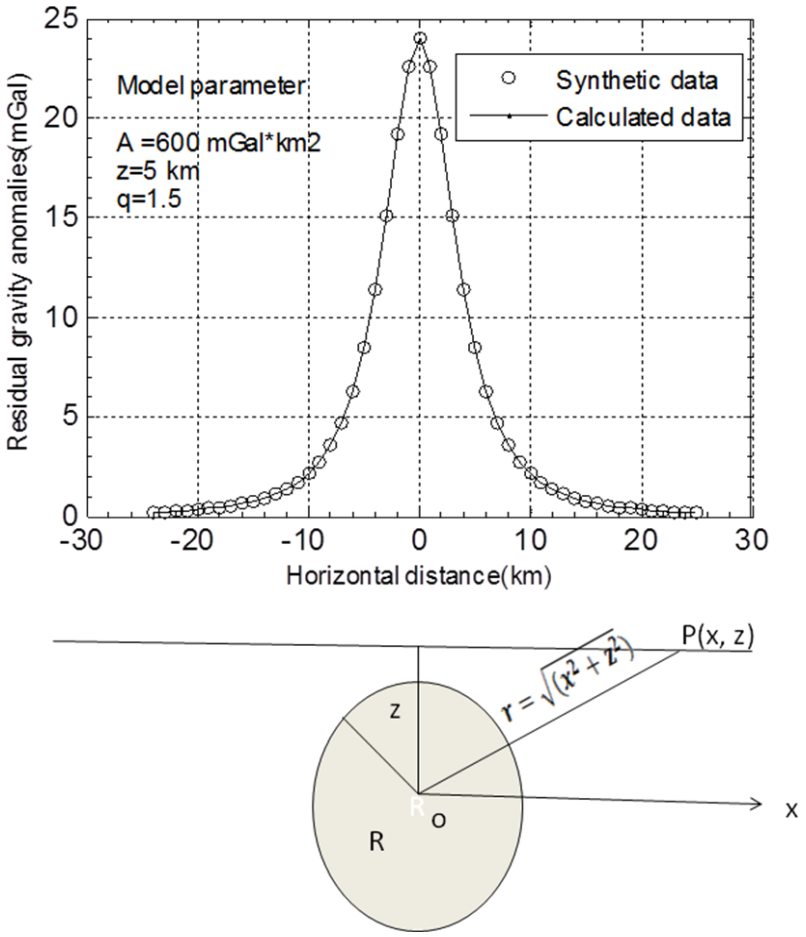
Model parameter
A =600 mGal*km2
z=5 km
q=1.5
Synthetic data
Calculated data
Residual gravity anomalies(mGal)
Horizontal distance(km)
25
20
15
10
5
0
-30
-20
-10
0
10
20
30
P(x, z)
r = √(x² + z²)
z
R
O
R
x

Figure 2(b)

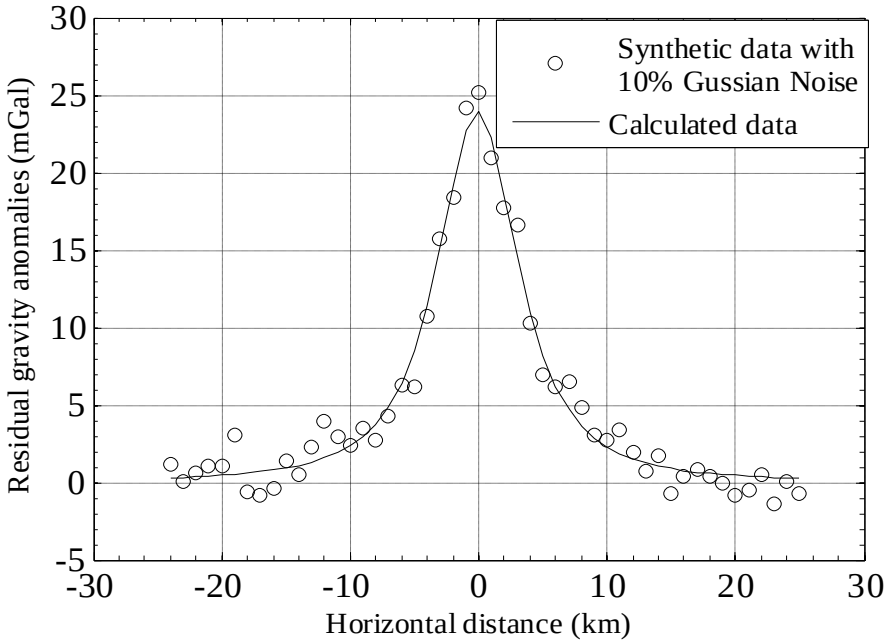
Synthetic data with
10% Gussian Noise
Calculated data
Residual gravity anomalies (mGal)
Horizontal distance (km)
30
25
20
15
10
5
0
-5
-30
-20
-10
0
10
20
30

Figure 3(a)

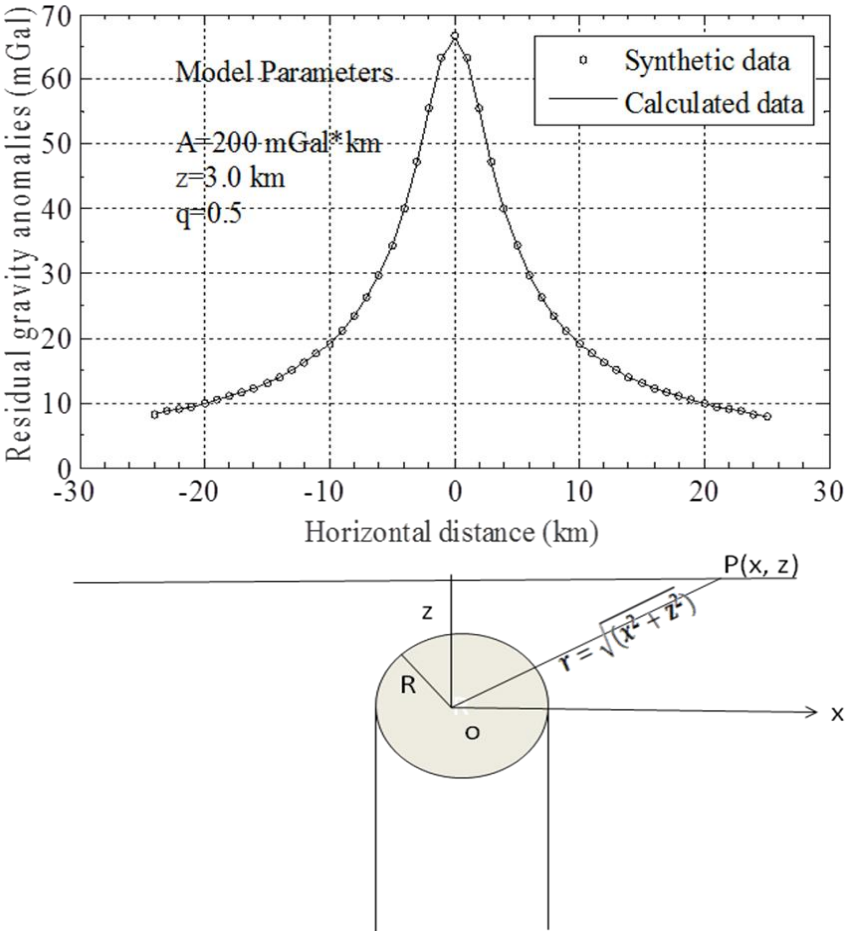
Residual gravity anomalies (mGal)
Horizontal distance (km)
Model Parameters
A=200 mGal*km
z=3.0 km
q=0.5
Synthetic data
Calculated data
P(x, z)
z
R
r = √(x² + z²)
x
o

Figure 3(b)

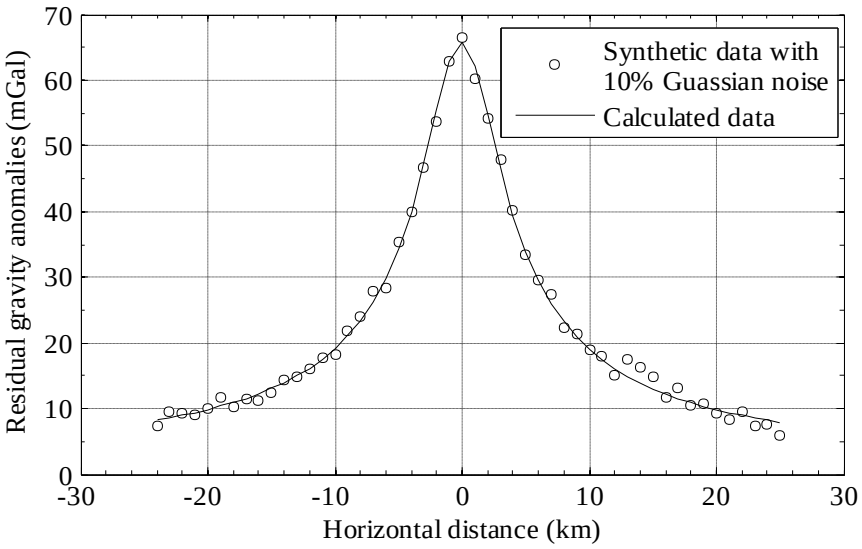
Residual gravity anomalies (mGal)
Horizontal distance (km)
Synthetic data with
10% Guassian noise
Calculated data
70
60
50
40
30
20
10
0
-30
-20
-10
0
10
20
30

Figure 4

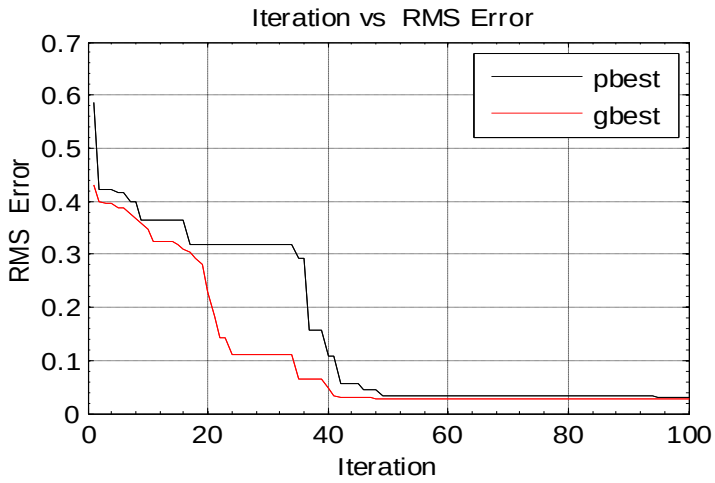
Iteration vs RMS Error
RMS Error
Iteration
pbest
gbest
0.7
0.6
0.5
0.4
0.3
0.2
0.1
0
0
20
40
60
80
100

Figure 5

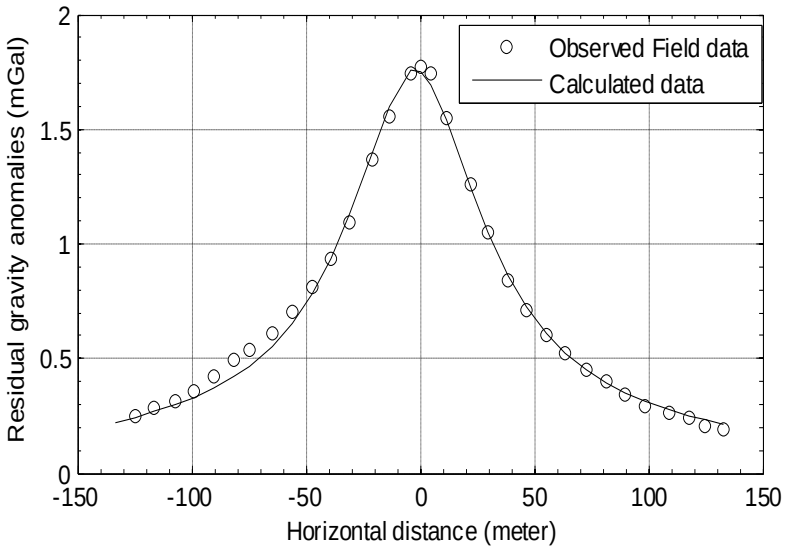
Observed Field data
Calculated data
Residual gravity anomalies (mGal)
Horizontal distance (meter)
2
1.5
1
0.5
0
-150
-100
-50
0
50
100
150

Figure 6

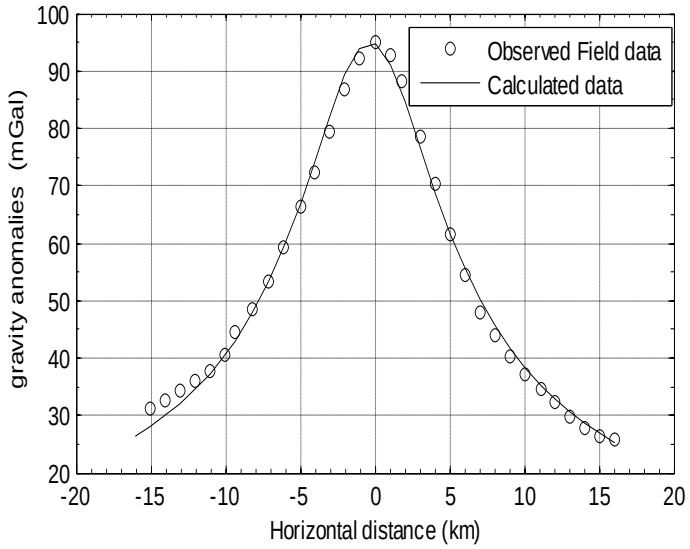
Observed Field data
Calculated data
gravity anomalies (mGal)
Horizontal distance (km)
100
90
80
70
60
50
40
30
20
-20
-15
-10
-5
0
5
10
15
20

579 Table 1

Gravity data description	Weighting factor	$c_1 = 1.0$, $c_2 = 1.0$	$c_1 = 1.2$, $c_2 = 1.2$	$c_1 = 1.4$, $c_2 = 1.4$	$c_1 = 1.6$, $c_2 = 1.6$	$c_1 = 1.8$, $c_2 = 1.8$	$c_1 = 2.0$, $c_2 = 2.0$
		RMS Error					
Synthetic spherical body	w = 0.4	0.004899	0.002899	0.00014	0.000907	0.000853	0.000861
	w = 0.7	0.002532	0.000118	0.000013	0.000087	0.000187	0.000247
	w = 0.9	0.005215	0.000118	0.000063	0.000379	0.000167	0.002695
Synthetic vertical Cylindrical body	w = 0.4	0.004892	0.003231	0.000327	0.000835	0.000704	0.000932
	w = 0.7	0.001913	0.000318	0.000011	0.000065	0.000207	0.000511
	w = 0.9	0.003259	0.000551	0.000189	0.000183	0.001265	0.002747

Table 2

(a) Optimized Parameters, converged iteration and RMS error in the inversion of synthetic gravity anomaly over a spherical source model.

Z (km)	A (mGal*km^2)	q	g_0 (mGal)	x_0 (km)	Iteration	RMS Error (%)
4.99883	550	1.5	24.0	-1.89×10^{-3}	100	0.000405
4.9999	660.31	1.5	24.0	2.39×10^{-5}	200	0.000015
5.00	610.15	1.5	24.0	-1.44×10^{-6}	300	0.000000
5.00	604.36	1.5	24.0	3.3×10^{-13}	400	0.000000
5.00	604.10	1.5	24.0	8.17×10^{-16}	500	0.000000

(b) Optimized Parameters, converged iteration and RMS error in the inversion of synthetic gravity anomaly with 10% white Gaussian noise over a spherical source model.

z (km)	A (mGal*km^2)	q	g_0 (mGal)	x_0 (km)	Iteration	RMS Error (%)
4.5	605.49	1.5	24	$-6.95\text{X}10^{-2}$	100	0.174890
4.5	603.99	1.5	24	$-6.81\text{X}10^{-2}$	200	0.174885
4.5	550.32	1.5	24	$-6.86\text{X}10^{-2}$	300	0.174883
4.5	601.42	1.5	24	$-6.86\text{X}10^{-2}$	400	0.174883
4.5	680.0	1.5	24	$-6.85\text{X}10^{-2}$	500	0.174883

Table 3

(a) Optimized Parameters, converged iteration and RMS error in the inversion of synthetic gravity anomaly over a vertical cylindrical source model.

Z (km)	A (mGal*km)	q	g_0 (mGal)	x_0 (km)	Iteration	RMS Error (%)
3.015	182.31	0.5	66.33	-4.4×10^{-3}	100	0.001743
3.016	185.92	0.5	66.33	-3.7×10^{-4}	200	0.001635
3.016	192.59	0.5	66.33	-2.74×10^{-10}	300	0.001633
3.015	162.15	0.5	66.33	-7.98×10^{-11}	400	0.001633
3.016	169.00	0.5	66.33	-6.58×10^{-11}	500	0.001633

(b) Optimized Parameters, converged iteration and RMS error in the inversion of synthetic gravity anomaly with 10% white Gaussian noise over a vertical cylindrical source model.

z (km)	A (mGal*km)	q	g_0 (mGal)	x_0 (km)	Iteration	RMS Error (%)
3.02	167.33	0.5	65.81	-3.95×10^{-2}	100	0.036732
2.99	160.38	0.5	66.33	1.36×10^{-2}	200	0.036968
3.02	161.74	0.5	65.88	-4.52×10^{-2}	300	0.036672
30.2	160.35	0.5	65.88	-4.50×10^{-2}	400	0.036672
3.02	198.67	0.5	65.88	-4.50×10^{-2}	500	0.036672

Table 4

(a) Optimized Parameters, converged iteration and RMS error in the inversion of field gravity anomaly over Mobrun sulphide ore body.

z (km)	A (mGal*km^2)	q	g_0 (mGal)	x_0 (km)	Iteration	RMS Error (%)
31	58.08	0.77	1.7781	-2.99078	100	0.027149
31	59.55	0.76	1.1156	-3.02429	200	0.027163
31	58.00	0.76	1.7826	-2.13091	300	0.027125
31	59.03	0.77	1.7826	-2.15033	400	0.027124
30	59.99	0.77	1.7992	-2.15013	500	0.027124

(b) Comparative results over Mobrun field example from various methods and GPSO.

Parameter	Grant and West (1965)	Euler deconvoltuion (Roy et al., 2000)	Fast interpretation Method	Tuned- PSO Method
Z(m)	30	29.44	33.3	30.0
q	-	0.77	0.78	0.77
A(mGal)	-	-	59.1	60.0

Table 5

(a) Optimized Parameters, converged iteration and RMS error in the inversion of field gravity anomaly over West Senegal (Louga area) anomaly.

z (km)	A (mGal*km)	q	g_0 (mGal)	x_0 (km)	Iteration	RMS Error (%)
4.90	549.44	0.52	94.83	-2.60×10^{-1}	100	0.027065
4.90	550.0	0.53	94.80	-2.56×10^{-1}	200	0.026552
4.91	549.57	0.53	94.79	-2.45×10^{-1}	300	0.026552
4.91	547.66	0.53	94.79	-2.42×10^{-1}	400	0.026551
4.91	545.30	0.53	94.79	-2.39×10^{-1}	500	0.025551

(b) Comparative results of various methods over West Senegal (Louga area) anomaly.

Parameter	New fast least square method (Essa, 2014)	Tuned-PSO method
z (km)	4.94	4.92
q	0.53	0.53
A (mGal)	545.68	545.30